

Exploring Dark Matter Properties from Cosmic-ray Physics

Ding Ran



Cao Qing-Hong, DR, Xiang Qian-Fei, arXiv:2006.12767

Yuan Guan-Wen , Chen Zhan-Fang , Shen Zhao-Qiang , Guo Wen-Qing ,
DR, Huang Xiaoyuan , Yuan Qiang, arXiv:2106.05901

第15届TeV物理工作组学术研讨会, 2021.07.18-21

Outline

- Introduction
- Exploring Sub-MeV DM from xenon electron direct detections
- Constraining WIMP annihilations from the EHT Observations of M87*

Introduction

● DM candidates



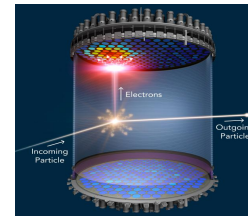
● DM detections

Cosmic-Ray (CR) physics



indirect detection

direct detection



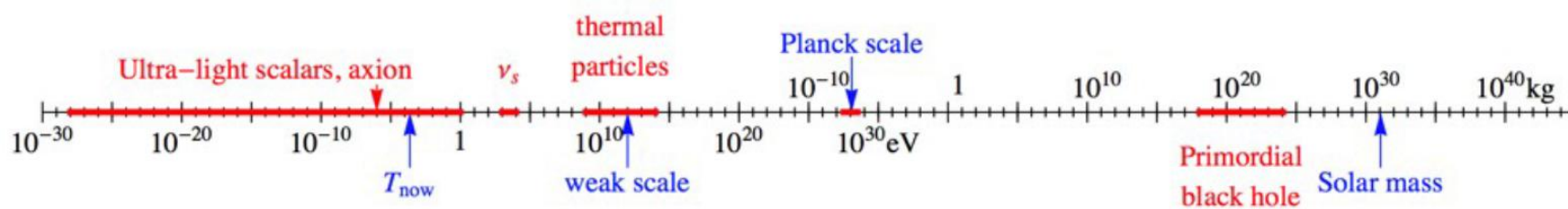
SM DM

SM DM

collider detection



©G. Bertone and T. P. Tait



- Theoretical motivation of light DM

- Dark photon mediator, milli-charged DM, freeze-in DM, Strongly Interacting, MDM/EDM.....

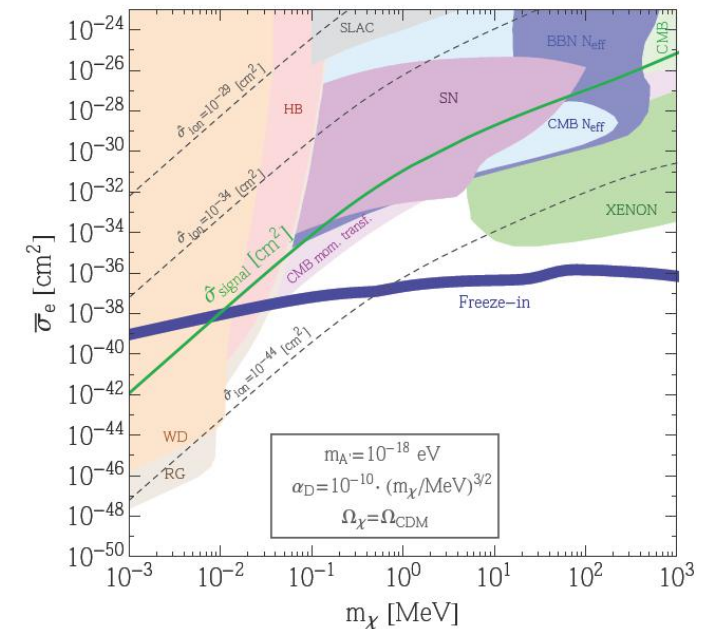
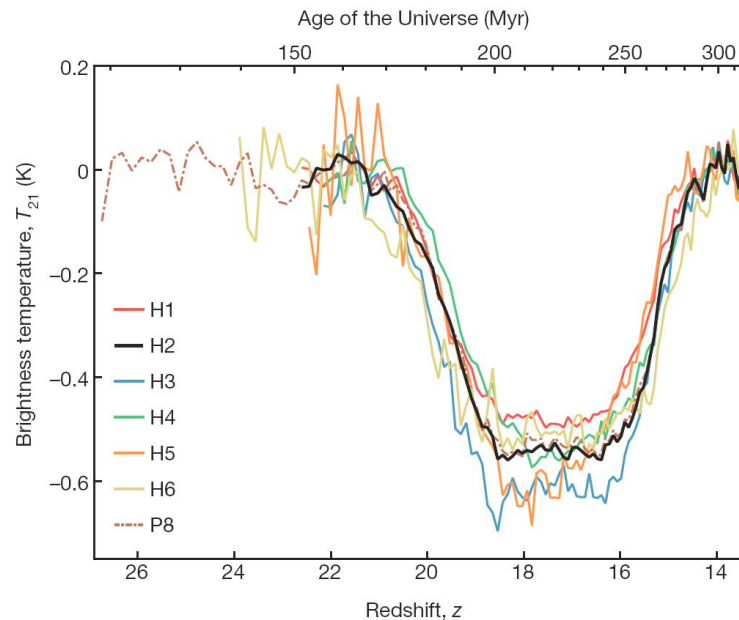
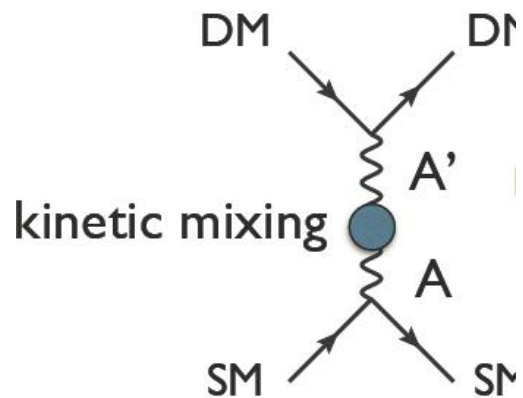
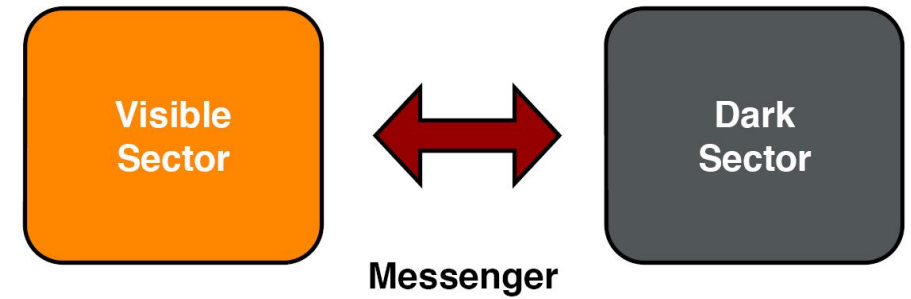
L. J. Hall, K. Jedamzik, J. March-Russell, and S. M. West, arXiv:0911.1120

R. Essig, J. Mardon, and T. Volansky, arXiv:1108.5383

X. Chu, T. Hambye, and M. H. G. Tytgat, arXiv:1112.0493

S. Knapen, T. Lin, and K. M. Zurek, arXiv:1709.07882

R. Barkana, N. J. Outmezguine, D. Redigolo and T. Volansky, arXiv:1803.03091



B. Holdom, Phys. Lett. 166B, 196 (1986)

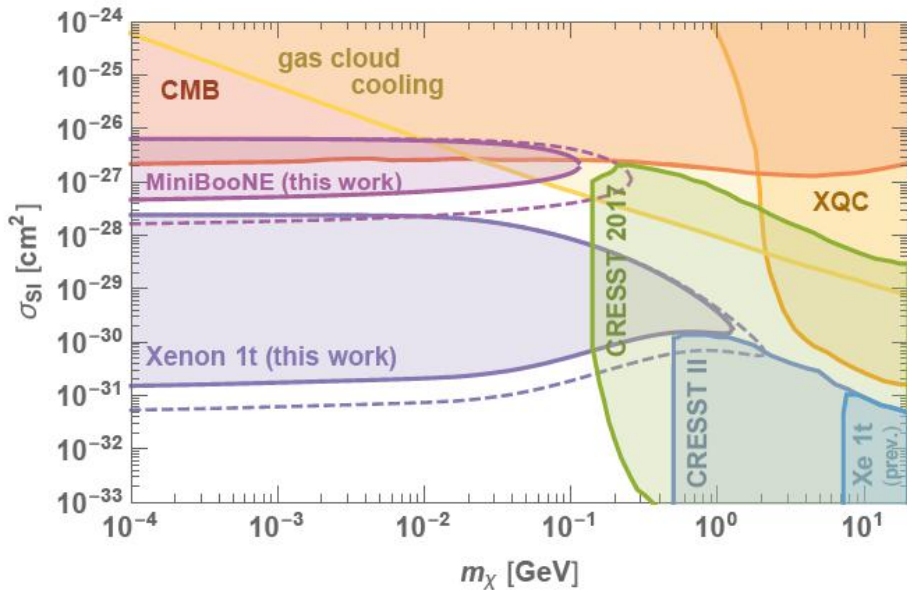
Exploring Sub-MeV DM from xenon electron direct detections

- CR-boosted DM

- A fraction of DM in Milky Way halo could be accelerated to high velocities, allowing for sensitivity to very light DM.

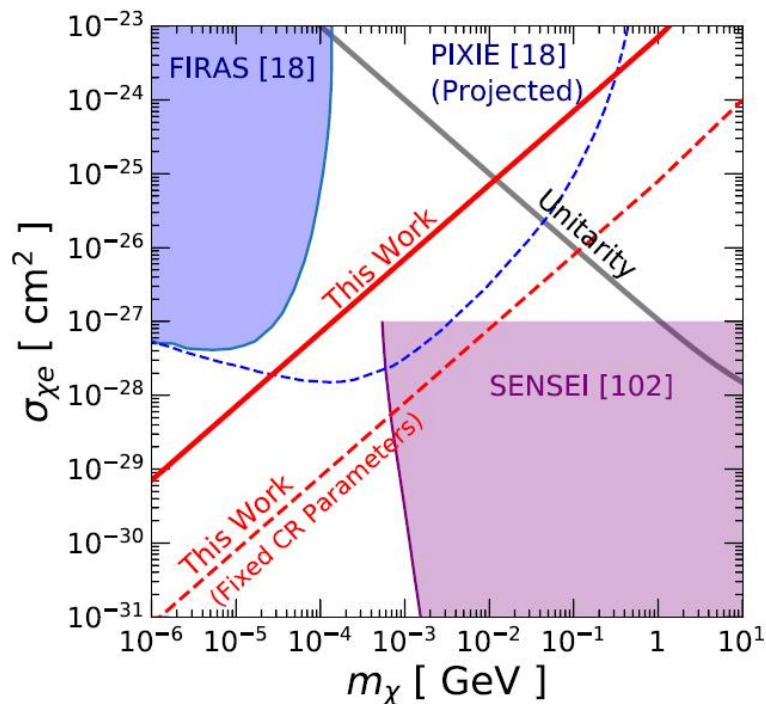
- DM-nucleon direct detection

T. Bringmann & M. Pospelov, arXiv:1810.10543



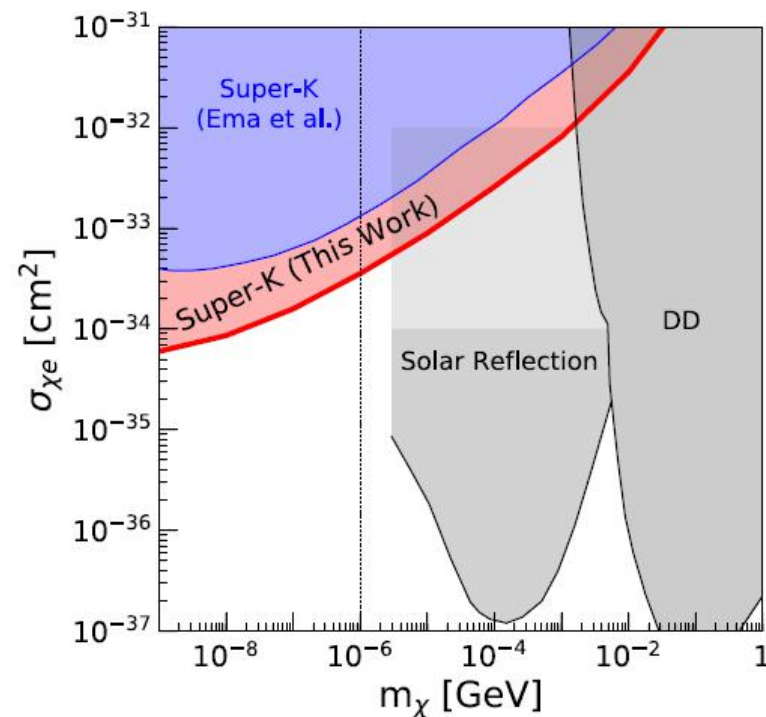
- Reverse direct detection

C. V. Cappiello, K. C. Y. Ng & J. F. Beacom, arXiv:1810.07705

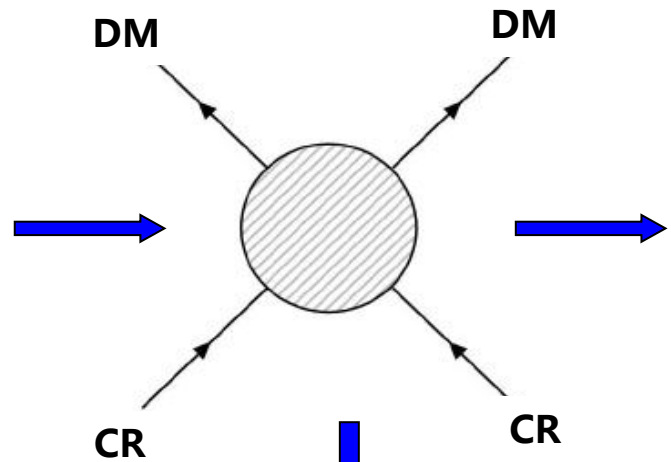
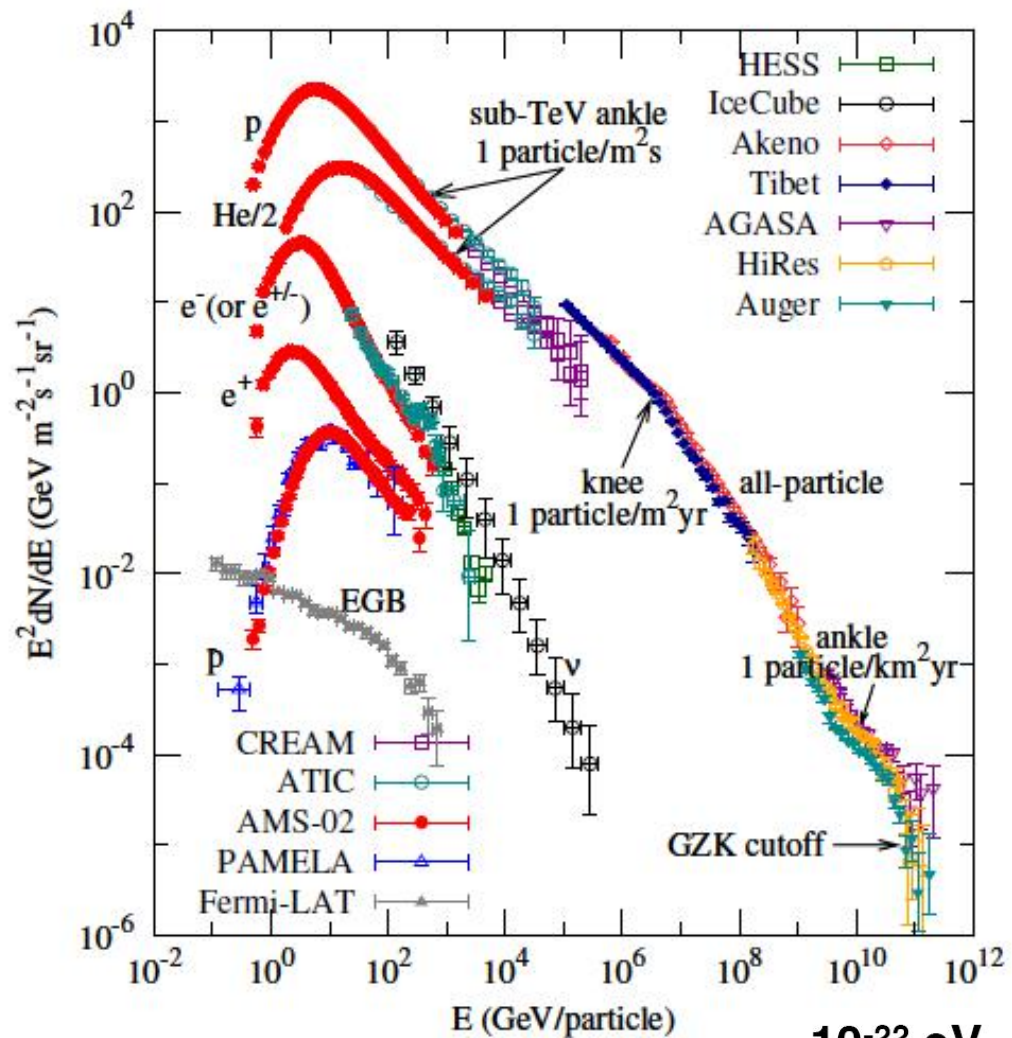


- Neutrino experiments

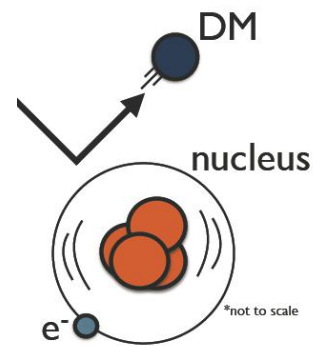
C. Cappiello & J. F. Beacom, arXiv:1906.11283



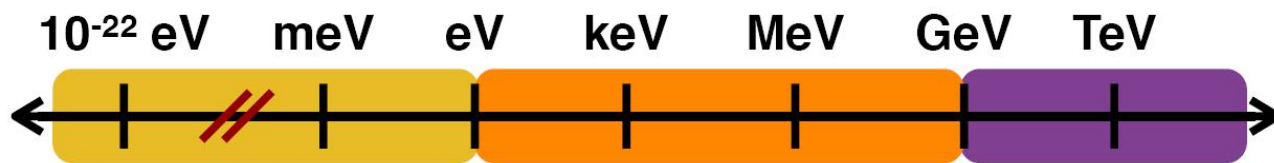
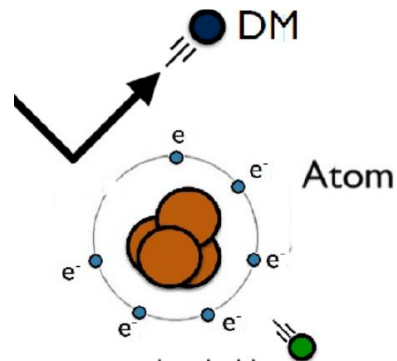
- We consider the constraints from DM-electron scattering.



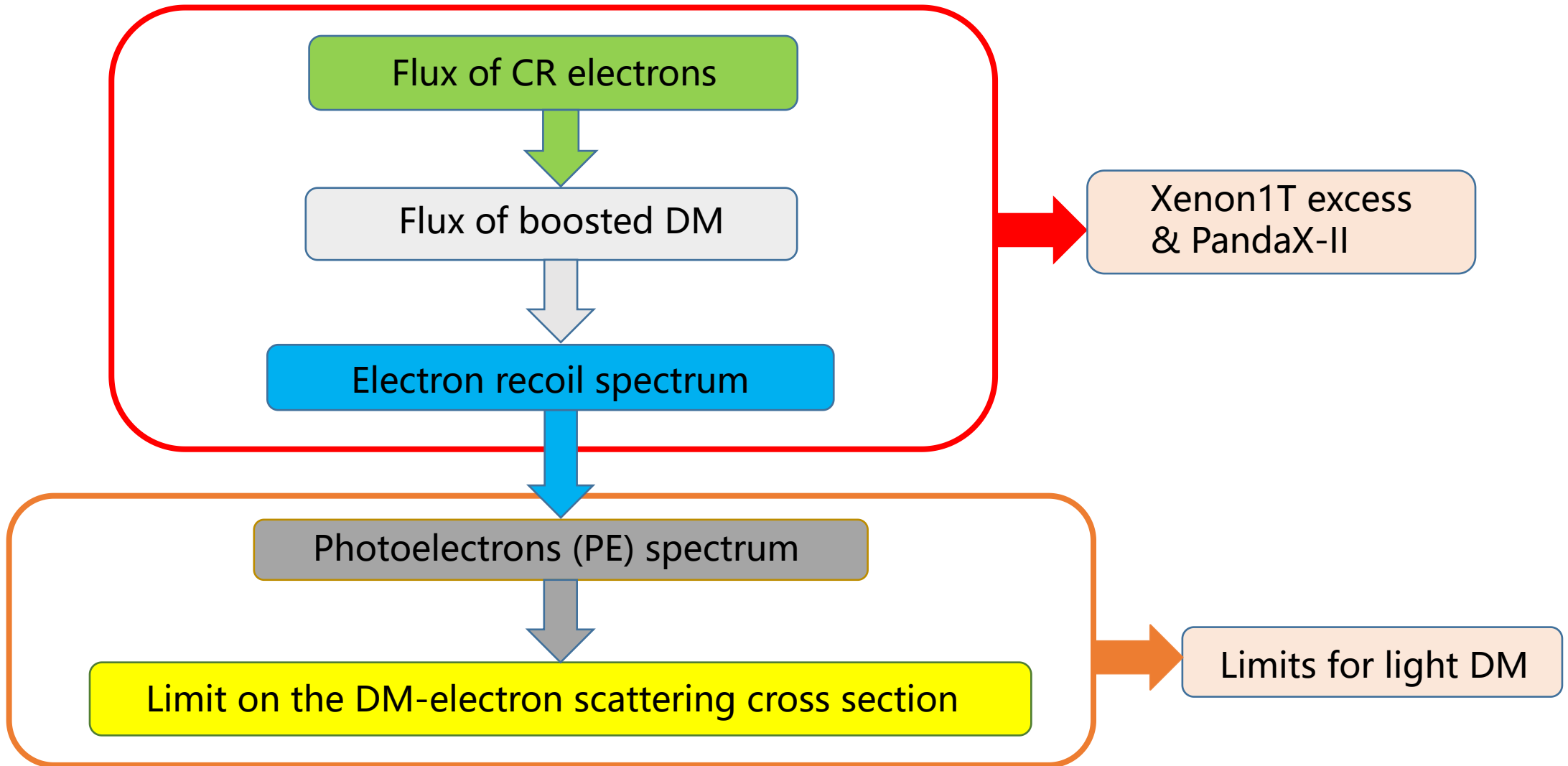
DM-nucleon scattering



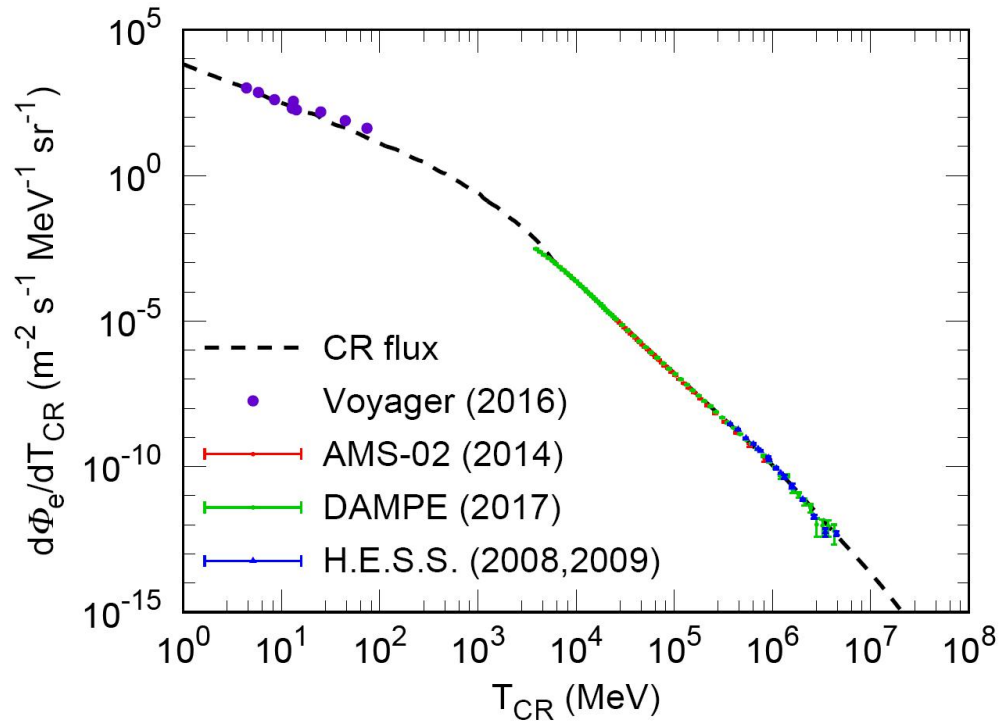
DM-electron scattering



- Calculation framework

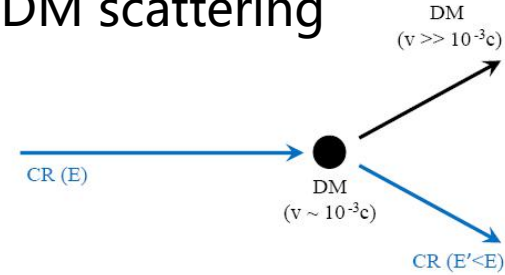


Flux of CR electrons



Flux of boosted DM

• Kinematics of CR-DM scattering



$$T_\chi = T_\chi^{\max} \frac{(1 - \cos \theta_{CM})}{2}, \quad T_\chi^{\max} = \frac{2m_\chi T_{CR} (T_{CR} + 2m_e)}{(m_e + m_\chi)^2 + 2T_{CR} m_\chi}$$

$$T_{CR}^{\min} = \left(\frac{T_\chi}{2} - m_e \right) \left(1 \pm \sqrt{1 + \frac{2T_\chi (m_e + m_\chi)^2}{m_\chi (2m_e - T_\chi)^2}} \right)$$

• Differential flux at Earth in terms of the CR energy

$$\frac{d\Phi_\chi}{dT_\chi} = D_{\text{eff}} \frac{\rho_\chi^{\text{local}}}{m_\chi} \int_{T_{CR}^{\min}}^{\infty} dT_{CR} \frac{d\Phi_e}{dT_{CR}} \frac{d\sigma_{\chi e}}{dT_\chi}$$

effective diffusion distance

$$D_{\text{eff}} \equiv \int \frac{d\Omega}{4\pi} \int_{l.o.s} dl$$

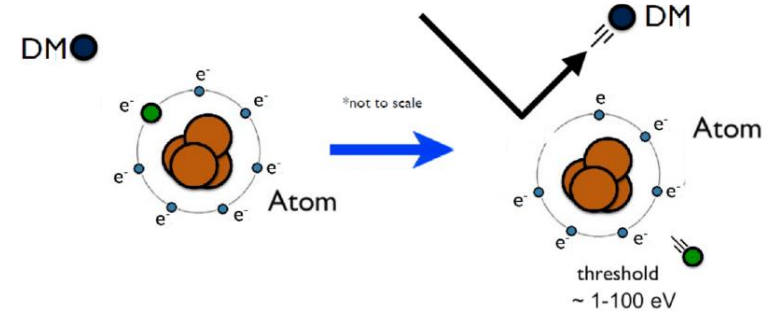
differential cross section

Electron recoil spectrum

- Differential scattering rate R. Essig, J. Mardon and T. Volansky, arXiv:1108.5383

$$\frac{d\langle\sigma_{ion}^{nl} v\rangle}{d \ln E_R} = \frac{\bar{\sigma}_e}{8\mu_{\chi e}^2} \int q dq |F_{DM}(q)|^2 |f_{ion}^{nl}(k', q)|^2 \eta(E_{\min})$$

Particle physics (points to $\bar{\sigma}_e$ and $|F_{DM}(q)|^2$)
quantum mechanics (points to $|f_{ion}^{nl}(k', q)|^2$)
CR physics (points to $\eta(E_{\min})$)



- ◆ Inverse mean speed function

$$\eta(E_{\min}) = \int_{E_{\min}} dE_{\chi} \Phi_{\text{halo}}^{-1} \frac{m_{\chi}^2}{p E_{\chi}} \frac{d\Phi_{\chi}}{dT_{\chi}} \xrightarrow{\text{non-relativistic limit}} \eta(v_{\min}) = \int_{v_{\min}} \frac{1}{v} f(v) d^3v$$

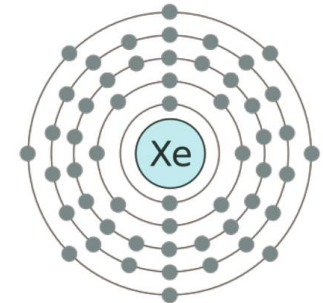
minimal DM energy required to trigger E_R (points to E_{\min})
background DM flux (points to Φ_{halo}^{-1})
flux of boosted DM (points to $\frac{d\Phi_{\chi}}{dT_{\chi}}$)

- ◆ Ionization from factor C. F. Bunge, J. A. Barrientos and A. V. Bunge (1993)

$$|f_{ion}^{nl}(k', q)|^2 = \frac{2k'^3}{(2\pi)^3} \sum_{\text{deg}} |f_{nl}(q)|^2 = \frac{(2l+1)k'^2}{4\pi^3 q} \int_{|k'-q|}^{|k'+q|} k dk \sum_{m=-l}^l |\chi_{nl}(k)|^2$$

radial wave functions: RHF method (points to $|\chi_{nl}(k)|^2$)

- Xe electron configuration



- Total differential ionization rate

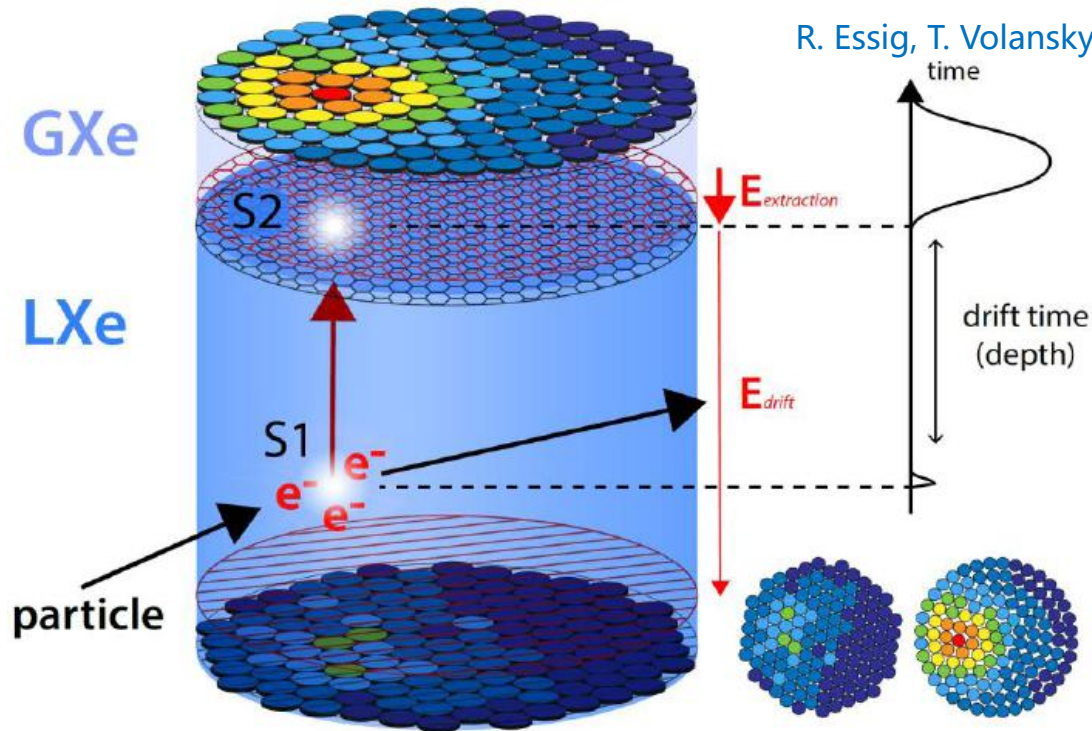
$$\frac{dR_{ion}}{d \ln E_R} = N_T \Phi_{\text{halo}} \sum_{nl} \frac{d\langle\sigma_{ion}^{nl} v\rangle}{d \ln E_R}$$

(5p⁶, 5s², 4d¹⁰, 4p⁶, 4s², 3d¹⁰, 3p⁶, 3s², 2p⁶, 2s², 1s²)

PhotoElectrons (PE) spectrum

R. Essig, A. Manalaysay, J. Mardon, P. Sorensen, and T. Volansky, arXiv:1206.2644

R. Essig, T. Volansky, and T.-T. Yu, arXiv:1703.00910



- Event rate for S2 signal responses

$$\frac{dN}{dS2} = \underbrace{T_{\text{exp}}}_{\text{Exposure}} \cdot \underbrace{\epsilon_{S2}}_{\text{trigger and acceptance efficiency}} \sum_{nl} \int dE_R \underbrace{\text{pdf}(S2|\Delta E_e)}_{\text{conversion probability of S2}} \underbrace{\frac{dR_{ion}^{nl}}{d \ln E_R}}_{\text{total differential ionization rate}}$$

deposit energy $\Delta E_e = E_R + |E_B^{nl}|$

- S1 (scintillation) signal: prompt scintillation photons

- S2 (ionization) signal: secondary scintillation photons from electroluminescence in Gxe due to drifted electrons

● Benchmark model

$$\mathcal{L} \supset g_\chi \bar{\chi} \gamma^\mu \chi A'_\mu + g_{\text{SM}} \bar{f} \gamma^\mu f A'_\mu + \frac{1}{2} m_{A'}^2 A'_\mu A'^\mu$$

ultralight A'

heavy A'

Dark photon mediator,
milli-charged DM

Z' -portal, leptophilic DM

$$g_\chi g_{\text{SM}} = g_\chi \kappa e = \epsilon e^2$$

◆ Constant cross section/matrix element

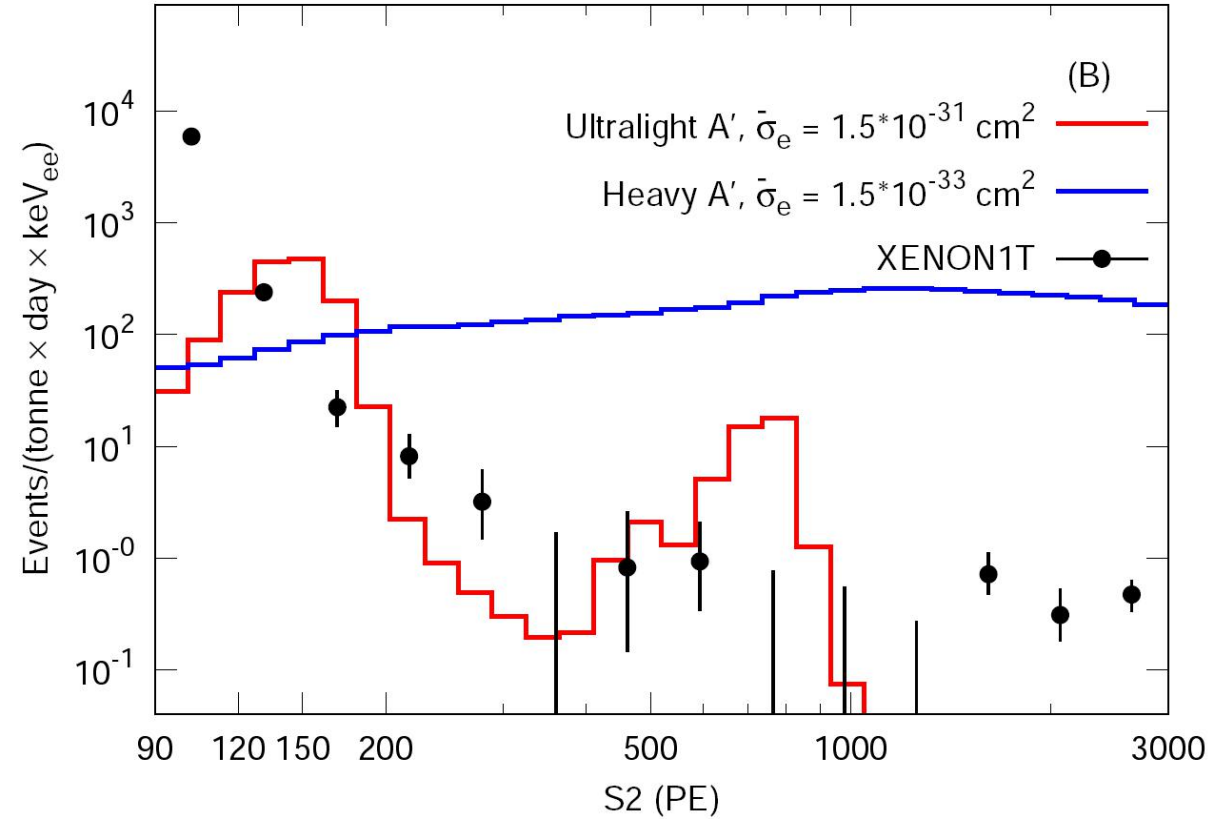
$$\frac{d\sigma_{\chi e}}{dT_\chi} = \bar{\sigma}_e \begin{cases} \frac{1}{T_\chi^{\text{max}}}, & \text{const } \sigma_{\chi e} \\ \frac{(m_\chi + m_e)^2}{(m_\chi + m_e)^2 + 2m_\chi T_{\text{CR}}} \frac{1}{T_\chi^{\text{max}}}, & \text{const } |\mathcal{M}|^2 \end{cases}$$

◆ Energy dependence in differential cross section

$$\frac{d\sigma_{\chi e}}{dT_\chi} = \bar{\sigma}_e \frac{(\alpha^2 m_e^2 + m_{A'}^2)^2 2m_\chi (m_e + T_{\text{CR}})^2 - T_\chi \left((m_e + m_\chi)^2 + 2m_\chi T_{\text{CR}} \right) + m_\chi T_\chi^2}{\mu_{\chi e}^2 4(2m_e T_{\text{CR}} + T_{\text{CR}}^2)(2m_\chi T_\chi + m_{A'}^2)^2}$$

$$\simeq \bar{\sigma}_e \begin{cases} \frac{2m_\chi (m_e + T_{\text{CR}})^2 - T_\chi \left((m_e + m_\chi)^2 + 2m_\chi T_{\text{CR}} \right) + m_\chi T_\chi^2}{4\mu_{\chi e}^2 (2m_e T_{\text{CR}} + T_{\text{CR}}^2)}, & \text{heavy } A' \\ \frac{\alpha^4 m_e^4}{16m_\chi^2 T_\chi^2} \frac{2m_\chi (m_e + T_{\text{CR}})^2 - T_\chi \left((m_e + m_\chi)^2 + 2m_\chi T_{\text{CR}} \right) + m_\chi T_\chi^2}{\mu_{\chi e}^2 (2m_e T_{\text{CR}} + T_{\text{CR}}^2)}, & \text{ultralight } A' \end{cases}$$

● XENON1T recoil spectrum

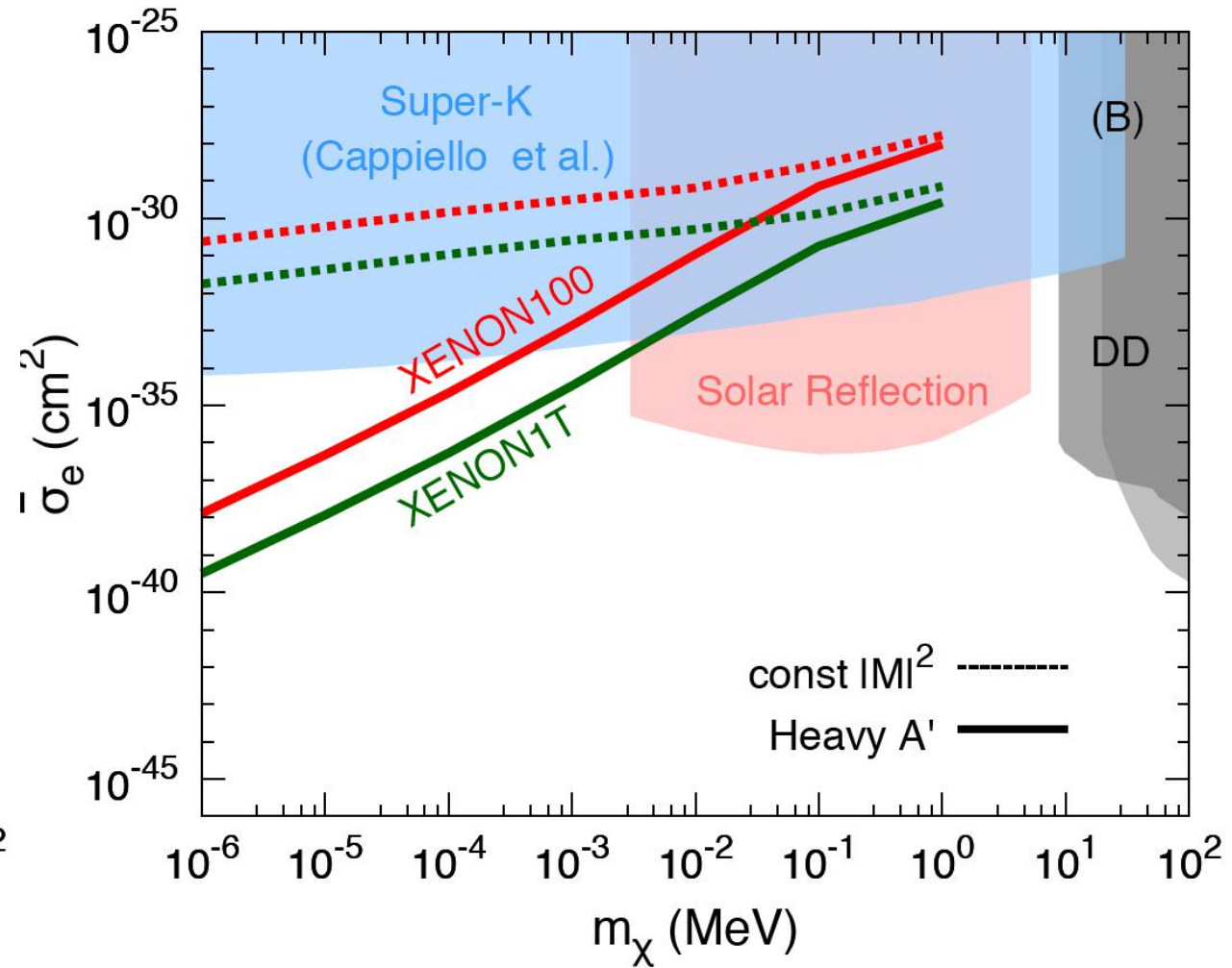
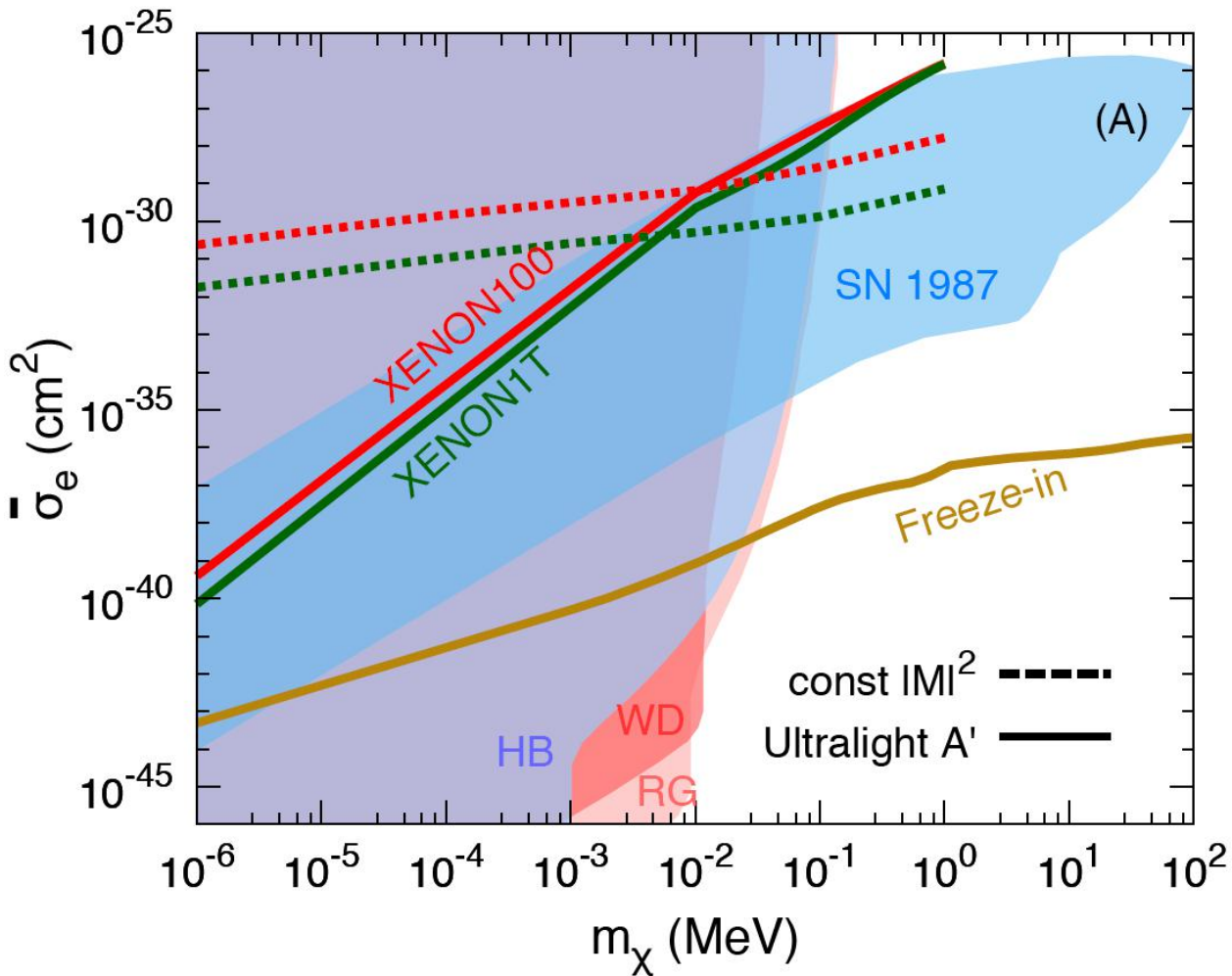


($T_{\text{exp}} = 22$ tonne-days)

Limit on the DM-electron scattering cross section

ultralight A'

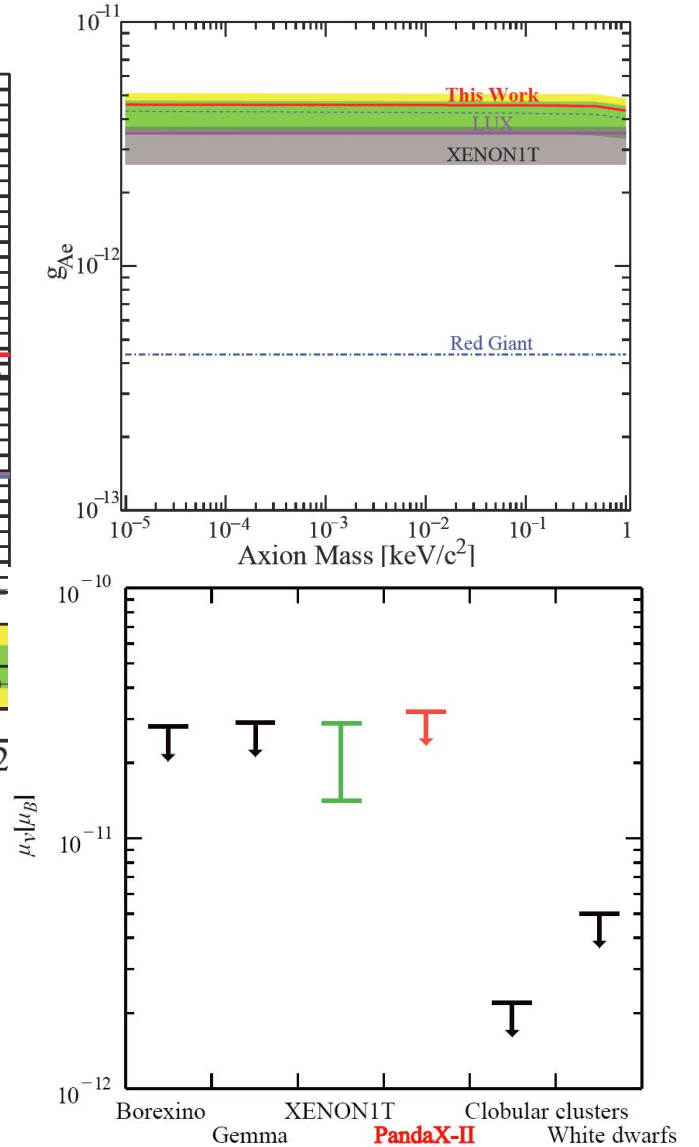
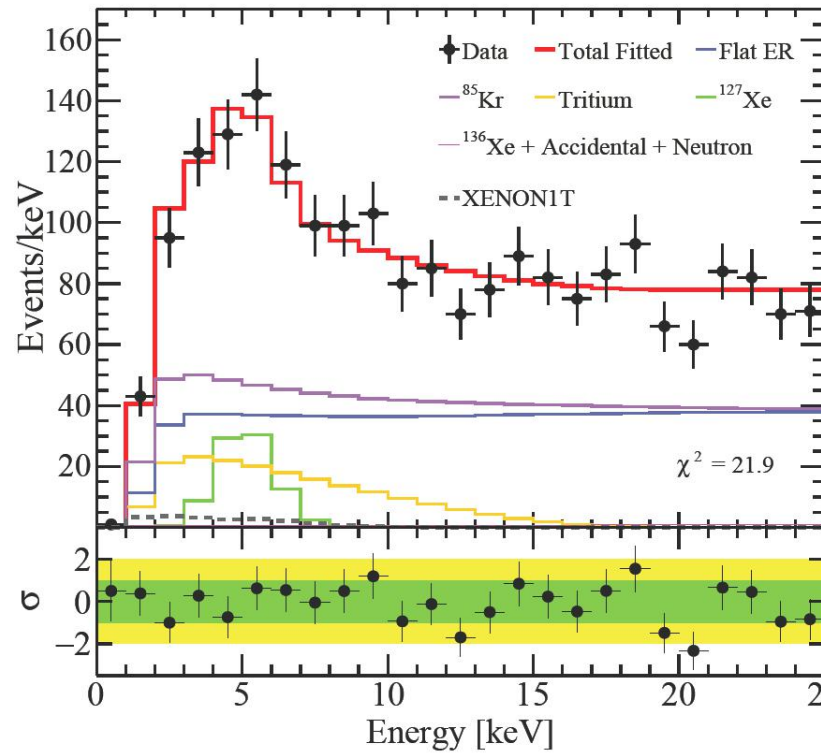
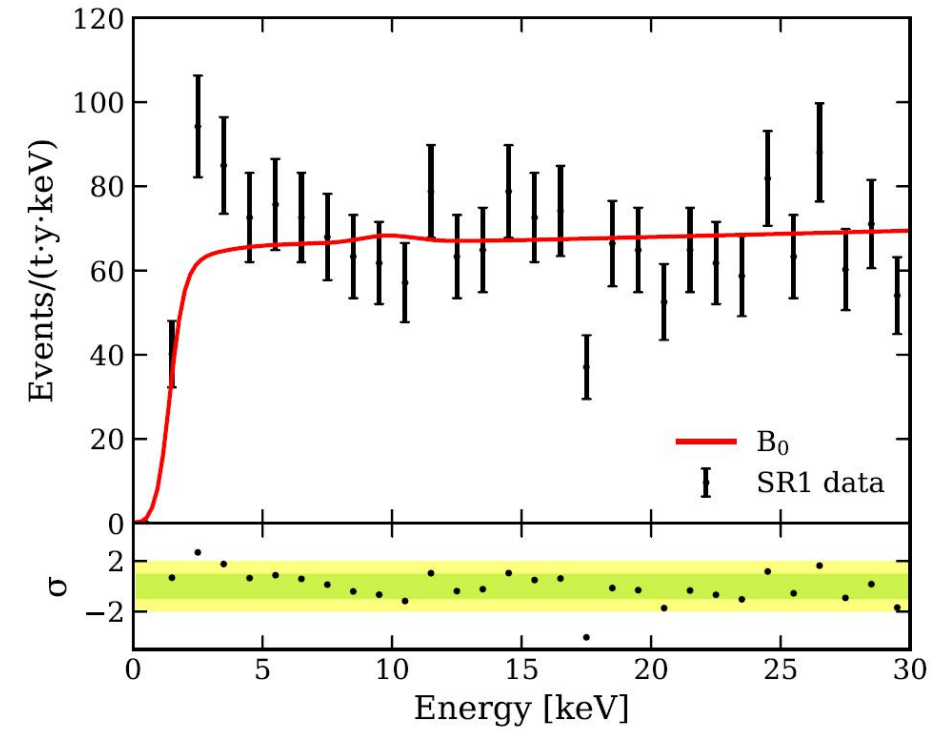
heavy A'



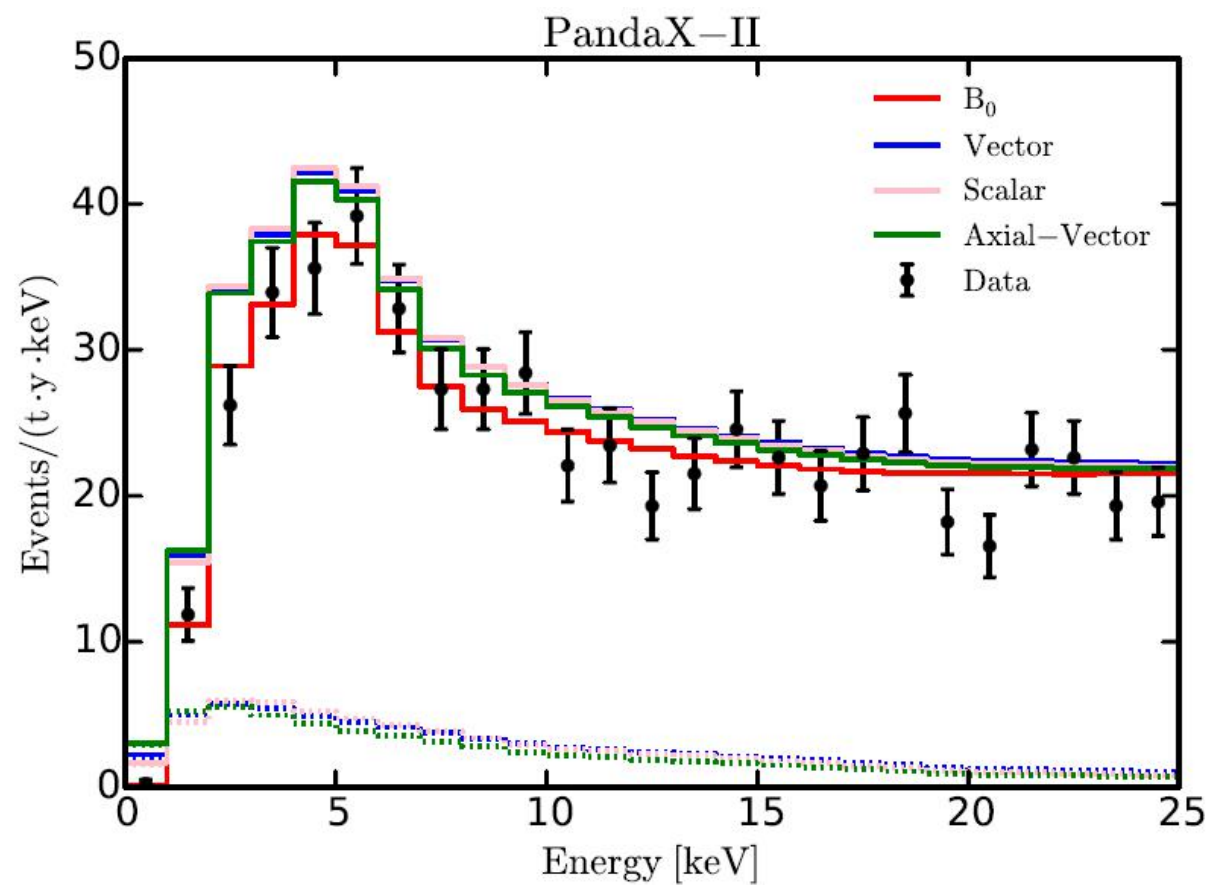
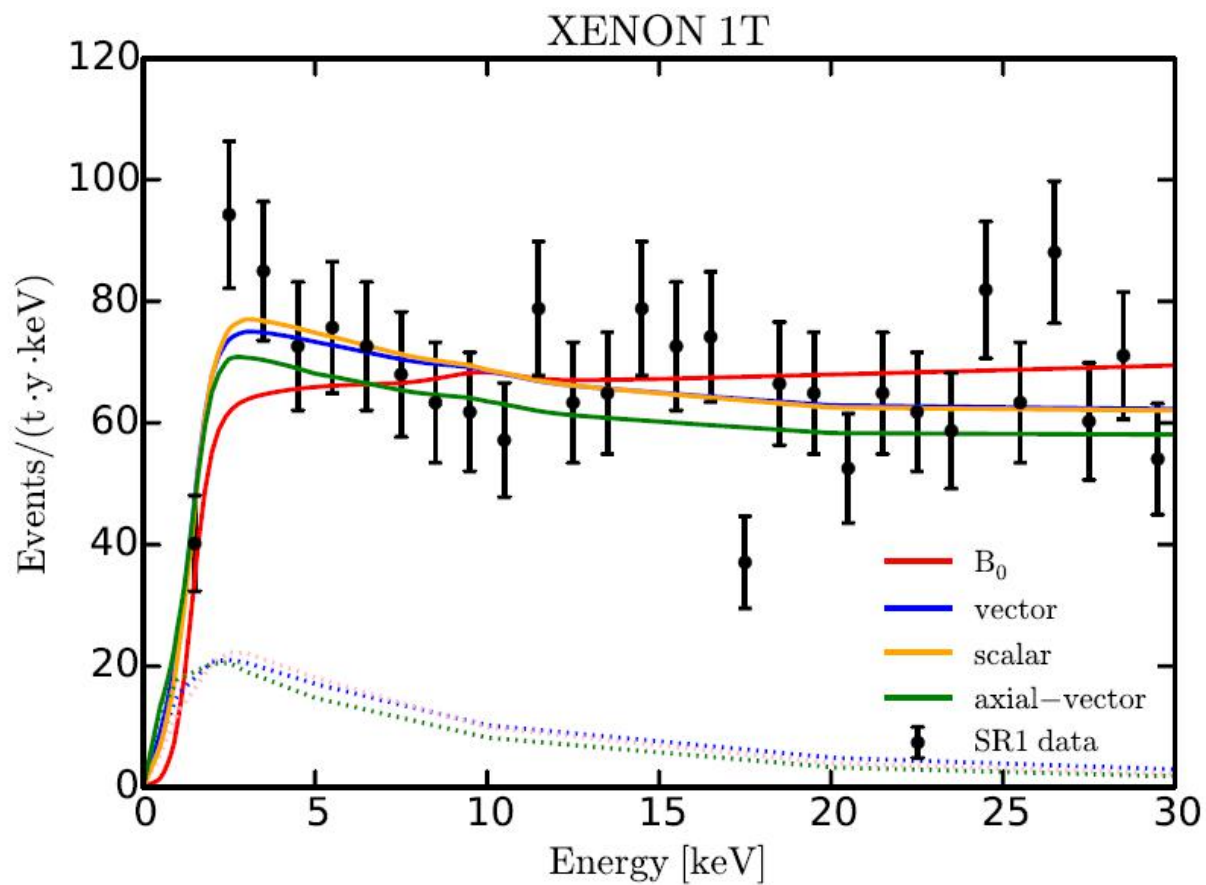
● XENON1T excess & PandaX-II constraint

XENON Collaboration, E. Aprile et al. arXiv:2006.09721

PandaX-II Collaboration, Xiaopeng Zhou et al. arXiv: 2008.06485



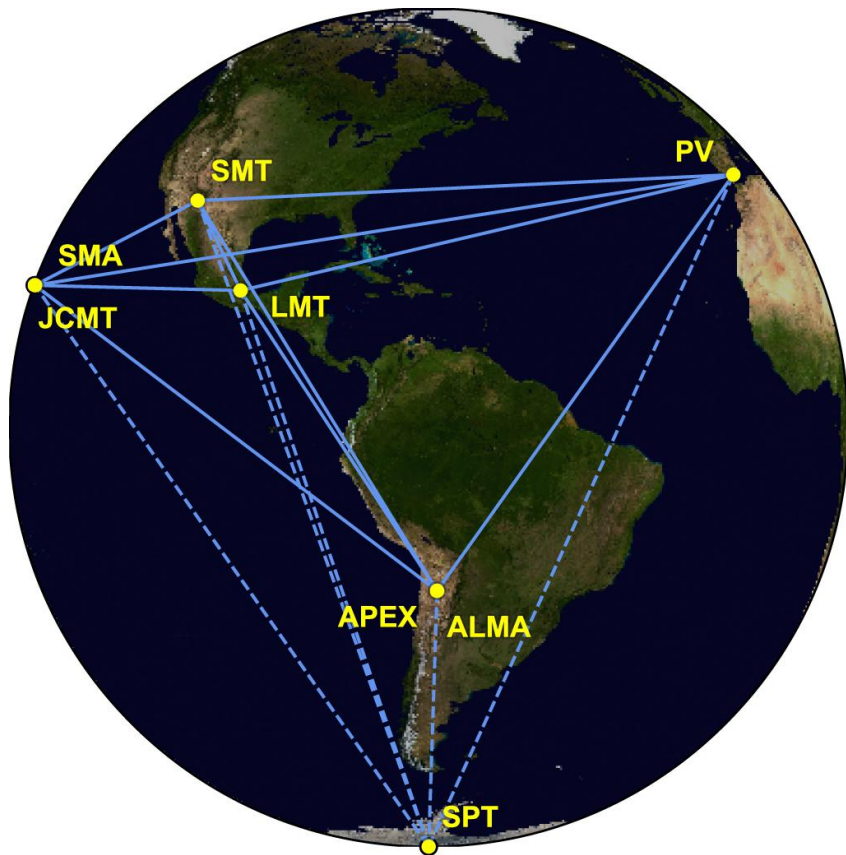
● Best fit spectra in XENON1T with PandaX-II constraint



Constraining WIMP annihilations from the EHT Observations of M87*

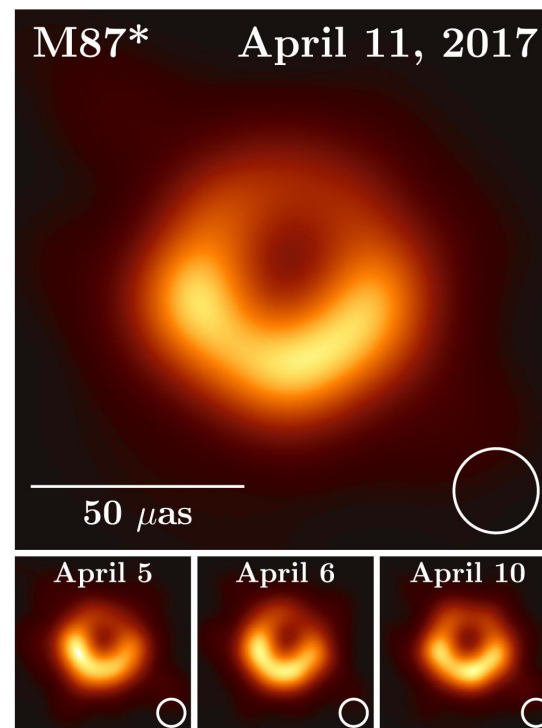
- The EHT project

- VLBI: Very Long Baseline Interferometry, an Earth-sized interferometer.
- EHT collaboration: focus on improving the capability of VLBI at short wavelengths.



- First image of a SMBH

EHT collaboration, *Astrophys. J. Lett.* 875 (2019) L1, [1906.11238]



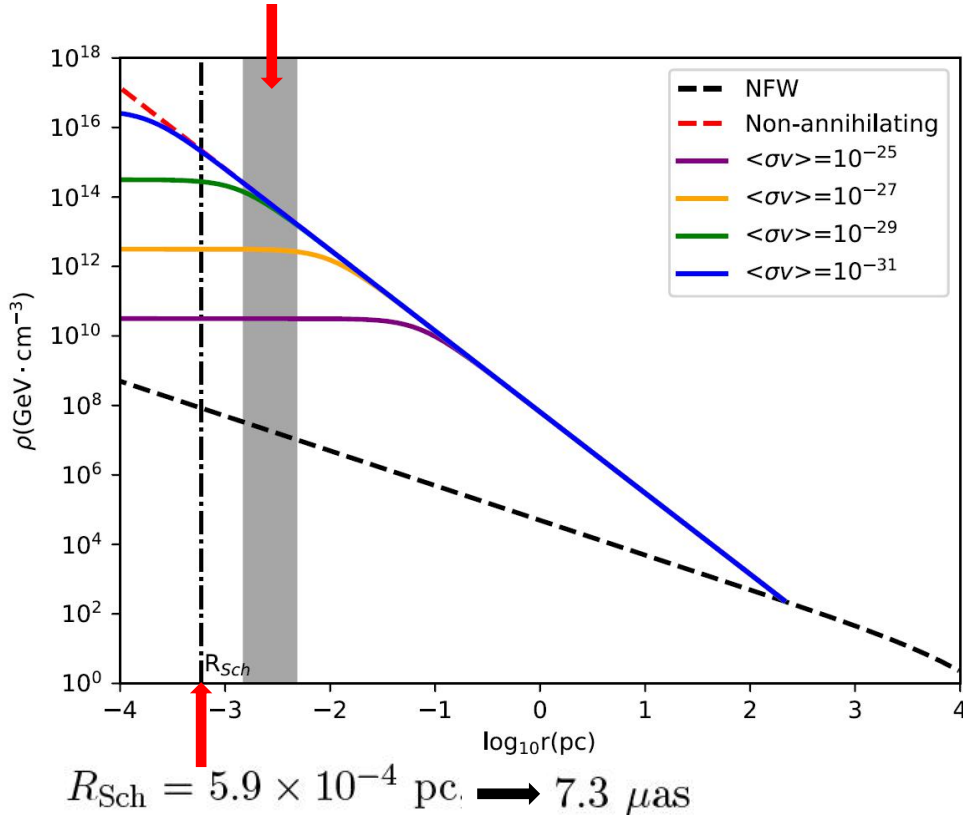
Symbol	Value	Property
M	$6.2 \times 10^9 M_{\odot}$	Compact object mass
D	16.9 Mpc	Compact object distance
$\nu_{\text{obs},0}$	230 GHz	Observing frequency

- DM spike model

- Adiabatic growth of SMBH will significantly enhance the DM density and form a spike structure.

P. Gondolo & J. Silk, PRL 83(1999) 1719{1722, [astro-ph/9906391]
 O. Y. Gnedin & J. R. Primack, PRL 93 (2004) 061302, [astro-ph/0308385]
 P. Ullio, H. Zhao & M. Kamionkowski, PRD 64 (2001) 043504, [astro-ph/0101481]
 R. Aloisio, P. Blasi & A. V. Olinto, JCAP 05 (2004) 007, [astro-ph/0402588]
 T. Lacroix, M. Karami, A. E. Broderick, J. Silk & C. Boehm, PRD 96 (2017) 063008, [1611.01961]

EHT observational areas



- DM density profile with Spike

$$\rho_{\chi}(r) = \begin{cases} 0 & r < R_{Sch}, \\ \frac{\rho_{sp}(r)\rho_{sat}}{\rho_{sp}(r)+\rho_{sat}} & R_{Sch} \leq r < R_{sp}, \\ \rho_{NFW}(r) & r \geq R_{sp}. \end{cases} \quad R_{sp} \simeq 220 \text{ pc}$$

↓ spike radius

- Saturate DM density

$$\rho_{sat} = m_{\chi} / \langle \sigma v \rangle t_{BH} \rightarrow \text{age of SMBH } t_{BH} = 10^9 \text{ yr}$$

- Synchrotron emission due to WIMP annihilations can be stringently constrained!

Calculation framework

R. Aloisio, P. Blasi & A. V. Olinto, JCAP 05 (2004) 007, [astro-ph/0402588]

T. Lacroix, M. Karami, A. E. Broderick, J. Silk & C. Boehm, PRD 96 (2017) 063008, [1611.01961]

$$S_{\text{syn}}(\nu) = \int d\Omega_{\text{obs}} \int_{l.o.s} dI_{\text{syn}}(\nu)$$

Specific intensity: radiative transfer equation

$$\frac{dI_{\text{syn}}(\nu, s)}{ds} = -\alpha(\nu, s)I_{\text{syn}}(\nu, s) + \frac{j_{\text{syn}}(\nu, s)}{4\pi}$$

relativistic Doppler effect and gravitational redshift

$$I_{\text{obs}}(\nu_{\text{obs}}) = \left(\frac{\nu_{\text{obs}}}{\nu_{\text{em}}}\right)^3 I_{\text{em}}(\nu_{\text{em}}) = g^3 I_{\text{em}}(\nu_{\text{em}})$$

emissivity

$$j_{\text{syn}}(\nu, r) = 2 \int_{m_e}^{M_\chi} dE \langle P_{\text{syn}} \rangle(\nu, E_e, B) n_e(r, E_e)$$

$$P_{\text{syn}}(\nu, E_e, B, \theta_p) = \frac{\sqrt{3}e^3 B \sin \theta_p}{m_e c^2} F(\nu/\nu_c)$$

$B \sim 1 - 30 \text{ G}$

power of synchrotron emission

electron and positron energy spectrum

$$n_e(r, E) = \frac{4\pi p^2}{c} f_e(r, p)$$

outside accretion radius : propagation equation

$$-\frac{1}{r^2} \frac{\partial}{\partial r} \left[r^2 D \frac{\partial f_e}{\partial r} \right] + v \frac{\partial f_e}{\partial r} - \frac{1}{3r^2} \frac{\partial}{\partial r} (r^2 v) p \frac{\partial f_e}{\partial p} + \frac{1}{p^2} \frac{\partial}{\partial p} (\dot{p} p^2 f_e) = q(r, p)$$

source function

$$q(r, p) = \frac{c}{4\pi p^2} Q(r, E) = \frac{c}{4\pi p^2} \frac{\langle \sigma v \rangle \rho_\chi^2(r)}{2m_\chi^2} \sum_i \text{BR}_i \frac{dN_{e^\pm}^{\text{inj}}}{dE}(E)$$

annihilation rate

injection spectrum

inside accretion radius: integral analytic solution

$$f_e(r, p) = \int_r^{r_{\text{acc}}} \frac{Q_i(R_{\text{inj}}, p_{\text{inj}})}{v(R_{\text{inj}})} \left(\frac{R_{\text{inj}}}{R_{\text{Sch}}}\right)^{\frac{5}{2}} \left(\frac{p_{\text{inj}}}{p}\right)^4 dR_{\text{inj}}$$

injection momentum

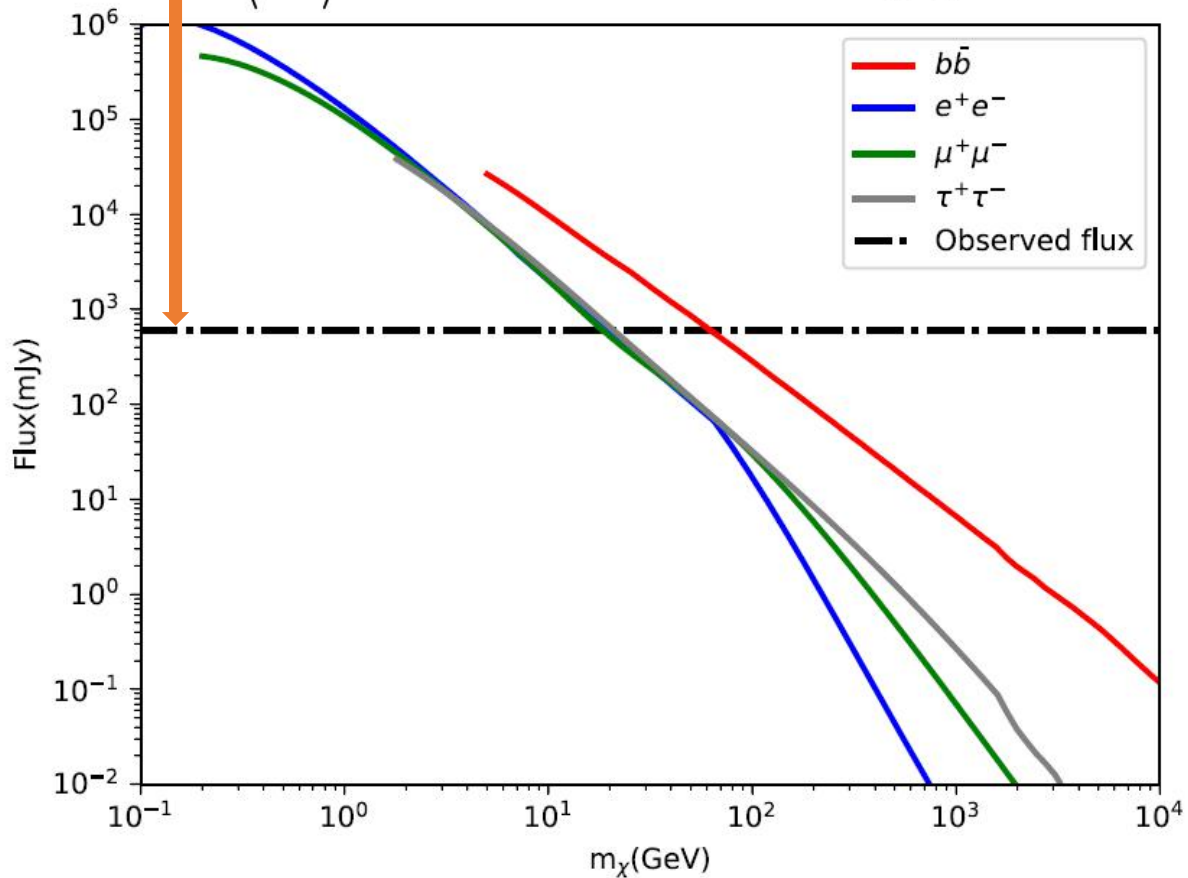
$$p_{\text{inj}}(R_{\text{inj}}; r, p) = p \left[\frac{k_0 R_{\text{Sch}}^{-\frac{1}{2}}}{c} R_{\text{inj}}^3 p \left(\frac{r}{R_{\text{inj}}} - 1\right) + \left(\frac{R_{\text{inj}}}{r}\right)^{\frac{1}{2}} \right]^{-1}$$

● Benchmark flux for four annihilation channels

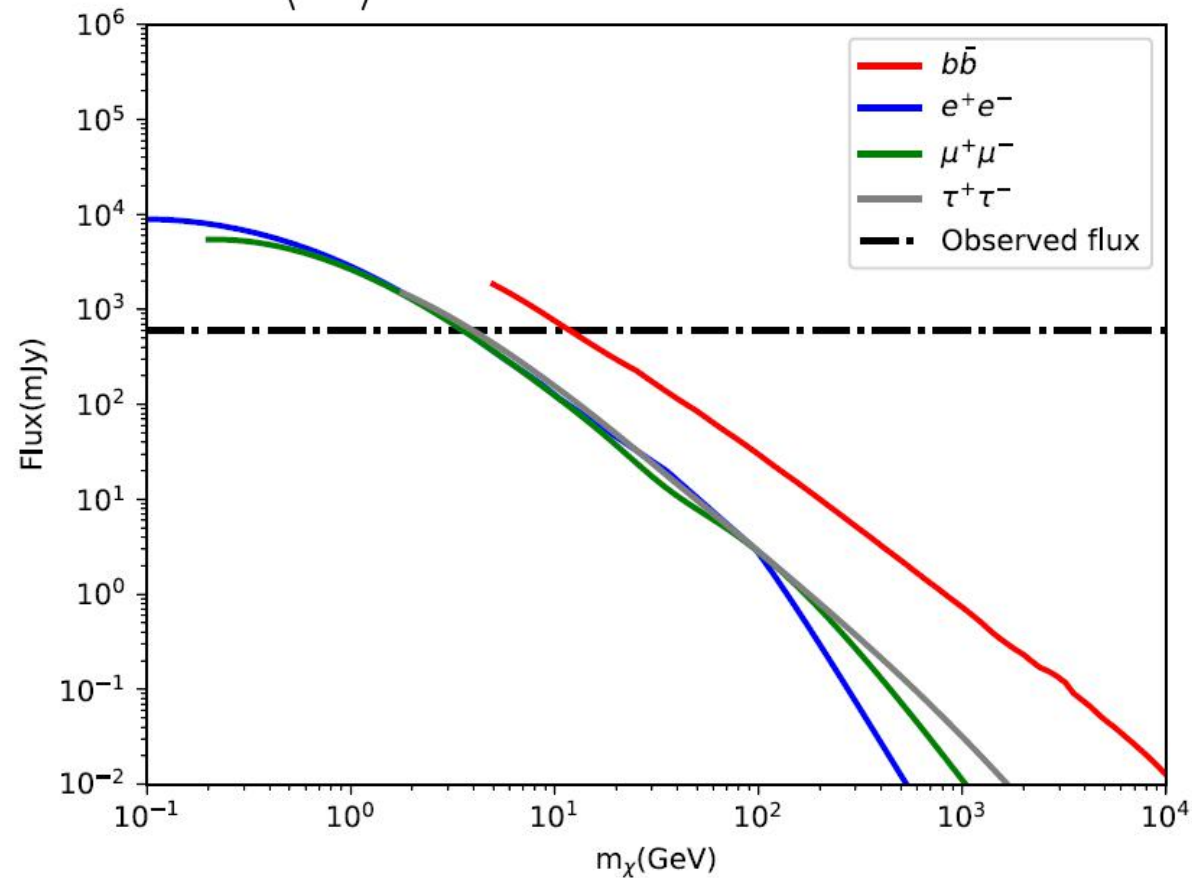
EHT collaboration, *Astrophys. J. Lett.* 910 (2021) L12, [2105.01169]

EHT collaboration, *Astrophys. J. Lett.* 910 (2021) L13, [2105.01173]

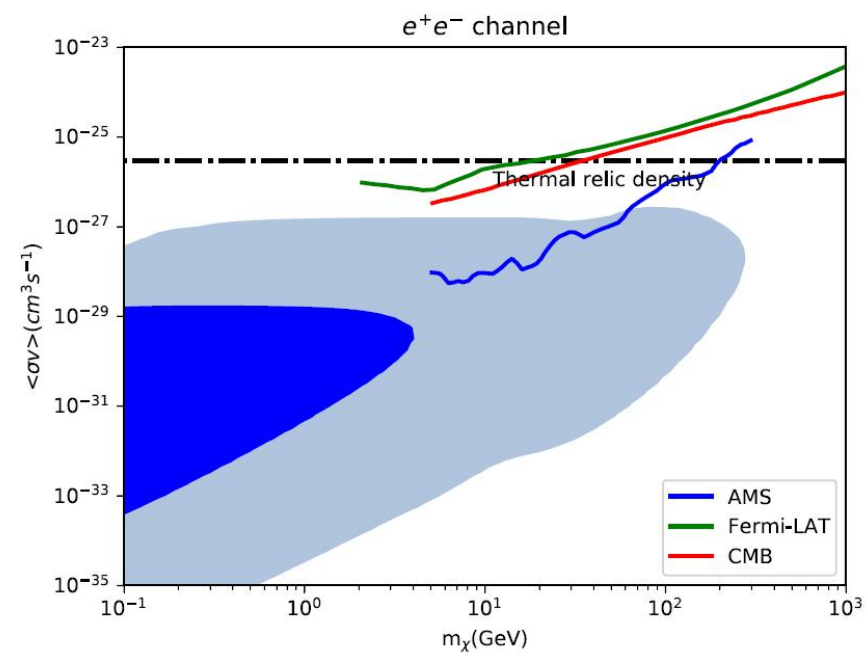
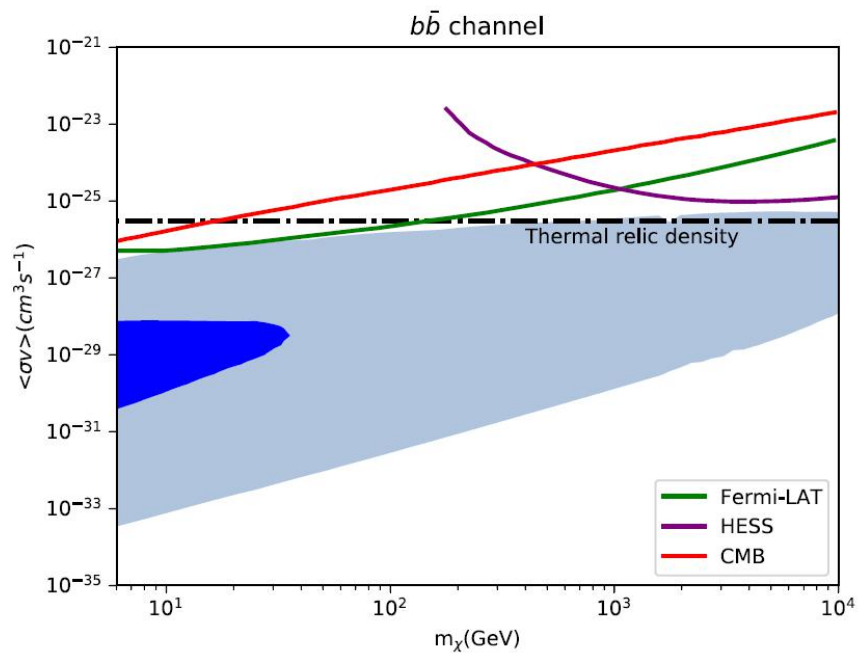
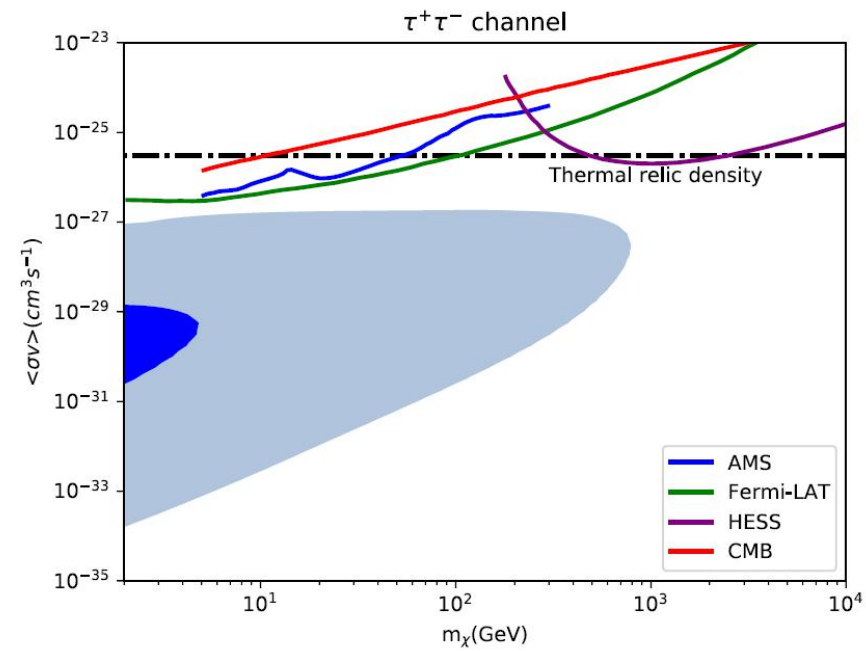
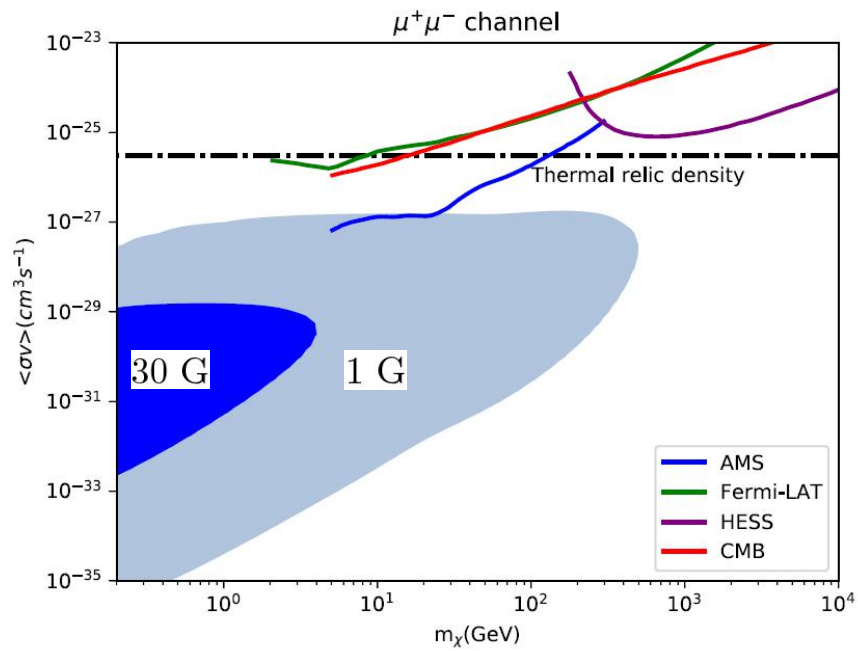
$\langle\sigma v\rangle = 10^{-32} \text{ cm}^3 \text{ s}^{-1}$ 1 G



$\langle\sigma v\rangle = 10^{-30} \text{ cm}^3 \text{ s}^{-1}$ 30 G



● Limits on WIMP annihilation cross sections



Thanks for your attention
Welcome to visit AHU!

